

Comparison of Transcriptomes and Sporulation of Two *Clostridium botulinum* A1 Strains



Virginia Ng and Wei-Jen Lin*

Biological Sciences Department, California State Polytechnic University, USA

Submission: March 20, 2018; Published: November 16, 2018

*Corresponding author: Wei-Jen Lin, Biological Sciences Department, California State Polytechnic University, 3801 W. Temple Ave. Pomona, CA 91768, USA

Abstract

Clostridium botulinum subtype A1 strains are one of the major causes of human botulism. Two of the genome-sequenced subtype A1 strains, Hall A and ATCC 3502, exhibit unique phenotypes in sporulation and botulinum neurotoxin (BoNT) production. Hall A, a hyper toxin producer used in BoNT/A production for medicinal and research purposes, is known to be deficient in sporulation, while ATCC 3502 is a laboratory strain capable of forming spores and producing a modest level of BoNT. Microarray-based transcriptomes were compared between these strains to identify key molecules contributing to these different phenotypes. Expression analysis showed that Hall A strain exhibited an increased expression level of the toxin cluster genes, which correlates to its hyper toxin production. Hall A also displayed a lower expression level of the sporulation initiation master regulator, Spo0A, and the forespore-specific Sigma F and Sigma G, which correlates to its poor sporulation phenotypes. In addition, Hall A showed a lowered expression level of CBO1120, a histidine sensor kinase that has been shown to activate sporulation by phosphorylating Spo0A. Further analysis of the sequences of CBO1120 showed an A to G base substitution at nucleotide position 661 resulting in a mutation of E221K. The differential expression of spo0A and CBO1120, as well as the critical point mutation identified in CBO1120, may imply that spo0A is not only poorly expressed in Hall A, its phosphorylation activation by the sensor histidine kinase may also be impaired. Overall, our genomic sequence and microarray analyses have brought insights into the genetic and physiological differences between the two *C. botulinum* Type A1 strains. The results may lead to further understanding of the sporulation process in *C. botulinum*.

Keywords: *Clostridium botulinum*; Microarray; Transcriptome; Sporulation; Neurotoxin

Introduction

Clostridium botulinum is a Gram positive, anaerobic bacterium with the ability to produce spores as well as Botulinum Neurotoxin (BoNT). Based on antigenicity and sequence similarities, BoNTs are grouped into seven serotypes (A - G) and several subtypes (e.g. A1 -A5). Most *C. botulinum* strains produce only one type of BoNTs; however, some strains may harbor a silent bont gene or are bivalent or, very rarely, trivalent [1]. Among the serotypes, only serotypes A, B, E, and F are known to cause botulism in humans. Studies of *C. botulinum* strains have been advanced by the availability of the genomic sequences and the gene annotation data. Phylogenetic analyses based on either 16S rRNA or COG both agree that the *C. botulinum* strains are diverse and may not coincide with the phylogeny of toxin types [2,3]. Analysis of the neurotoxin gene clusters revealed two major classes of bont clusters, orfX+ and HA+ clusters. The orfX+ clusters, correlating to the formation of a 300kDa neurotoxin complex of the 150kDa BoNT and the Non-Toxic Non-Hemagglutinin protein (NTNH), are found in strains of A1-A4, E and F; while HA+ clusters, correlating to the production of 300-900 kDa neurotoxin complex of various sizes of Hemagglutinins (HAs) and one molecule each of NTNH and BoNT, are found in A1, A5, B, C, D, and G serotypes/subtypes [4].

Interestingly, the bont/A1 is the only gene that is found in both HA+ and orfX+ clusters. It is hypothesized that the existence of bont/A1 gene on HA+ or orfX+ clusters was due to a recombination event [5-7]. The HA+ A1 cluster, consisting of ha17, ha70, ha33, botR, ntnh, and bont/A, is located around 900 kb position on the chromosome near the oppA/brnQ operon [4,8]. The orfX+ A1 cluster is found 48 kb upstream from the HA+ (B) cluster near the arsC operon in the A1(B) strain, NCTC 2916 [4]. Further analysis of the genomes of A1 subtypes showed a very similar genomic structure whereby the three assembled A1 genomes, ATCC 3502, Hall A, and ATCC 19397, as well as the partially assembled genome of an A1(B) subtype, NCTC 2916, shared over 90% core genes [3].

The synteny dot plot analyses also showed a close relationship of these A1 strains to all sequenced strains within the proteolytic Group I *C. botulinum* strains as well as *C. sporogenes* strain ATCC 15579 [3]. It has also been shown that the level of the neurotoxin production varied with strains as well as growth media [9, 10]. An excess of tryptophan decreased toxin production in *C. botulinum* serotype E [11], while an excess of arginine suppressed toxin and protease activity in *C. botulinum* strains Okra B and Hall A [12]. Further analysis showed that the expression of neurotoxin gene

cluster peaked at late-log to early stationary growth phase and is known to be regulated by both positive and negative regulatory elements [13]. BotR, encoded within the neurotoxin gene cluster, has shown to function as an alternative RNA polymerase sigma factor to activate the expression of the *ntnh-bont* and *ha* operons in a similar fashion as the TetR in *C. tetani* [14-16]. More recently, three Two-Component Systems (TCSs) were identified in subtype A1 strain Hall to positively control the transcription of the neurotoxin gene cluster, independently of BotR/A [17]. The HA+ A1 cluster was also found to be negatively regulated by a TCS, CBO0787/CBO0786, where CBO0786 was shown to bind to the promoters of *ha* and *ntnh-bont* operon [18]. A homologous TCS, CLC0842/CLC0843, was also identified in the subtype A1 strain Hall A [13]. In addition, two distinct *agr* quorum sensing systems were identified, among them, *agr-2* seems to control neurotoxin production in *C. botulinum* group I strains [19].

Although the sporulation process of *C. botulinum* is not well understood, several recent comparative genomic studies have shed some light on how it may work in *C. botulinum*. Unlike *Bacillus subtilis*, *C. botulinum* lacks genes encoding for Spo0B and Spo0F, the intermediates in the phosphorelay of the initiation process of sporulation [20]. Worner et al. [20] further identified a sensor histidine kinase, CBO1120, in *C. botulinum* ATCC 3502 that appeared to be able to directly phosphorylate Spo0A, although three additional orphan kinases (CBO0336, CBO0340, and CBO2762) may function similarly [20]. The expression of Spo0A and four sporulation-specific sigma factors in *C. botulinum* ATCC 3502 was analyzed by qPCR and the results showed slightly different expression patterns than those in *B. subtilis* [21]. Specifically, *spo0A* was expressed during the exponential phase, which may initiate the concomitant transcription of *sigF*, *sigE*, and *sigG* at the end of the exponential phase. The expression of *sigK* occurred at both early and late stages of sporulation, as evident by the early termination of sporulation in a *sigK* mutant [21,22]. Interestingly, the *sigF*, *sigE*, and *sigG* mutants appeared to impair *spo0A* expression, indicating the role of these sigma factors in early sporulation [23].

In addition, Dahlsten et al. [24] suggested that SigK may play an additional role in stress responses to cold and hyperosmotic conditions in *C. botulinum* ATCC 3502. A quorum sensing network identified as the accessory gene regulatory (*agr*) system is known to play a vital part in the virulence of methicillin-resistant *Staphylococcus aureus* [25]. Homologs to this *agr* system have been found in genomes of various *Clostridium* spp. In *C. difficile*, the *agr* genes have been shown to contribute to virulence [26]. In Group I *C. botulinum* and *C. sporogenes*, two *agrBD* loci were found, where *agr-1* may control sporulation and *agr-2* may mediate neurotoxin production [19]. To further characterize the sporulation process of *C. botulinum*, the global gene expression profiles (i.e. transcriptomes) were compared between two subtype A1 strains known to show unique phenotypes in sporulation and toxin production level. *C. botulinum* Hall A, a hyper toxin producer used in BoNT/A production for medicinal and research purposes, is known to be deficient in sporulation. While ATCC 3502 is a

laboratory strain with the capability to form spores and produce a modest level of BoNT. The aim of this study was to compare the transcriptomes between the two strains, ATCC 3502 and Hall A, in searching for distinctive expression patterns of molecules that may correlate to the sporulation and level of neurotoxin production. The results may lead to further understanding of sporulation in *C. botulinum*.

Materials and Methods

Bacterial strains and media

Clostridium botulinum strains, ATCC 3502, Hall A (aka Hyper Hall), and NCTC 2916 were grown in Cooked Meat Medium (CMM) for the bacterial stock and TPGY medium (5% Trypticase peptone, 0.5% Bacto peptone, 0.4% glucose, 2% yeast extract) for growth studies. Growth was performed at 37 °C in Hungate anaerobic tubes (Bellco Glass, Vineland, NJ). All procedures involving *C. botulinum* were performed using Biosafety Level 2 practices in a laboratory registered with the CDC Select Agent Program.

Cell collection and RNA purification

Bacterial growth was monitored for 120 hours with at least triplicate samples for the growth study. At least three independent studies were performed. Specifically, an overnight culture was inoculated to fresh TPGY tubes at a concentration that will yield a 0.03 optical density (OD at 600 nm) value. The tubes were incubated at 37 °C and the growth was monitored by OD at 600 nm for up to 120 hours. RNA was extracted from cells collected at 4, 6, and 8 hours after inoculation to represent the mid-log, late-log, and early-stationary phases of growth. In order to minimize RNase contamination, RNA procedures were performed with caution and used reagents of RNase-free and/or the highest grade possible, as well as RNase Away Reagent (Fisher, Pittsburgh, PA). At each time point of collection, RNA Protect Bacteria Reagent (Qiagen, Valencia, CA) was immediately added to the cell suspension at a 2:1 ratio to protect the RNA from degradation. This mixture was incubated at room temperature for 5 minutes followed by centrifugation at 6,000 rpm for 10 minutes. Cell pellets were stored at -80°C for no more than one week until RNA extraction. The RNA was extracted by the RNeasy Mini kit (Qiagen, Valencia, CA) following the manufacturer's instructions. The concentration and quality of RNA was determined by Nanophotometer (Implen, Westlake Viillage, CA).

Transcriptome analysis using microarray

The *C. botulinum* Version 2 microarray slides used in this study were kindly provided by the Pathogen Functional Genomics Resource Center (PFGRC) of J. Craig Venter Institute (JCVI, Rockville, MD). The "Microbial RNA Aminoallyl Labeling for Microarrays" protocol (SOP: M007 Rev. 2; pfgrc.jcvi.org/index.php/microarray/protocols.html) was followed for synthesizing cDNA and preparing the probes with Alexa Fluor Cy 3 and Cy 5 dyes (Invitrogen, Carlsbad, CA). Except for the reverse-dye experiments for quality control, cDNAs from strain ATCC 3502 were labeled with Cy 5, while cDNAs from Hall A were labeled with Cy 3 in this study. The "Hybridization of labeled DNA and

cDNA probes” protocol (SOP: M008 Rev. 2.1; pfgrc.jcvi.org/index.php/microarray/protocols.html) was used to hybridize the probes to the microarray slides. After hybridization, the washed microarray slides were scanned by GenePix® 4000B microarray scanner (Molecular Devices, Sunnyvale, CA) using GenePix® Pro 6.0 to capture the images. Scanned images (.tif) of the microarray slides were analyzed using the TM4 Suite (www.tm4.org), which encompasses four individual software tools: Spot Finder, Microarray Data Analysis System (MIDAS), Multi Experiment Viewer (MEV), and Microarray Data Manager (MADAM). Briefly, microarray spots were screened manually in Spot Finder and only the high-quality spots were exported to MIDAS where the data went through rigorous normalization and calibration steps such as the “LocFit Normalization (LOWESS)”, “Standard Deviation Regularization”, and “In-Slide Replicates Analysis” to avoid variations due to dye labeling bias, spot location bias, and slide-to-slide variations. At least two independent microarray data were analyzed for each time point.

Results

Growth curves vary slightly between strains

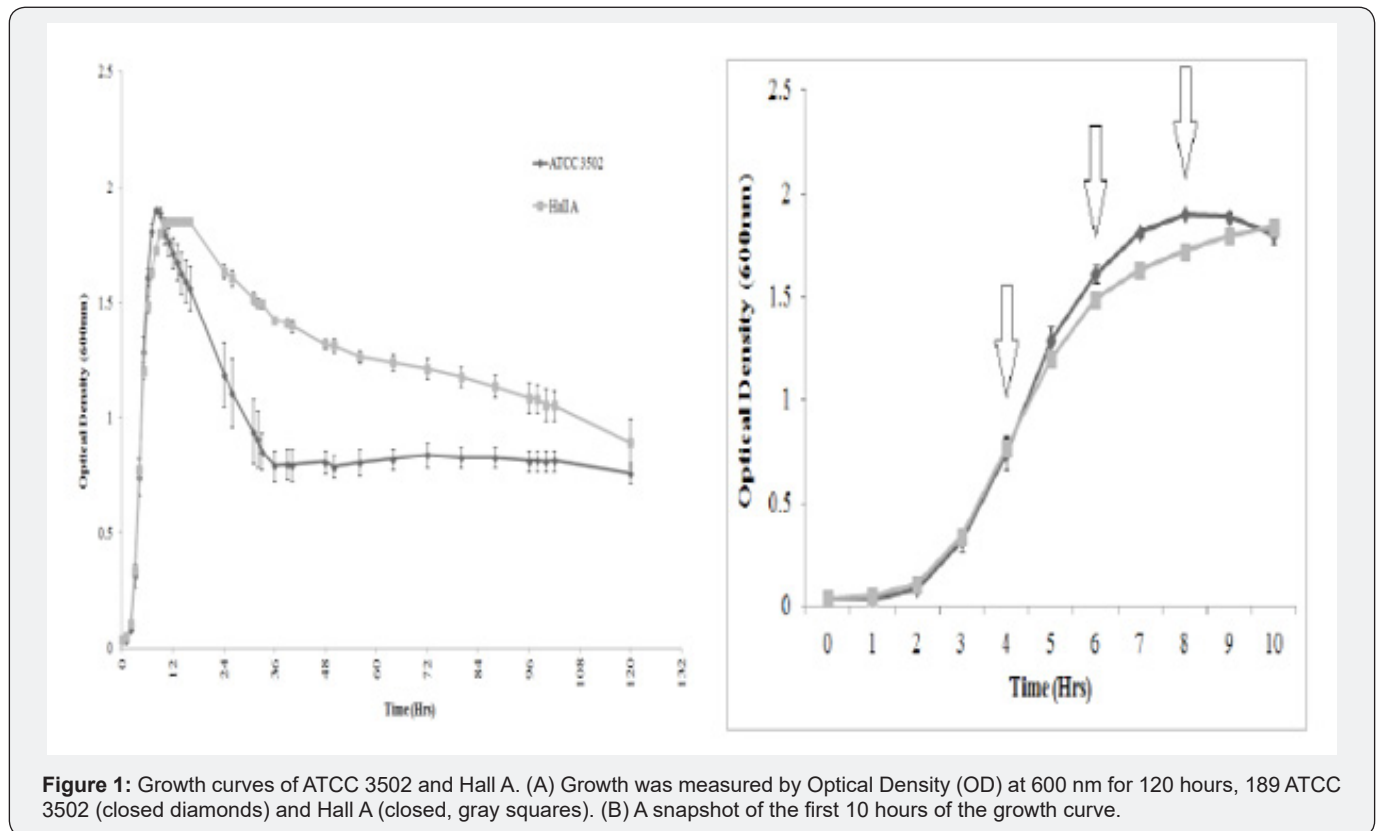


Figure 1: Growth curves of ATCC 3502 and Hall A. (A) Growth was measured by Optical Density (OD) at 600 nm for 120 hours, 189 ATCC 3502 (closed diamonds) and Hall A (closed, gray squares). (B) A snapshot of the first 10 hours of the growth curve.

The growth was compared between *C. botulinum* strains ATCC 3502 and Hall A. Both bacteria strains grew similarly in TPGY medium. Growth started to show about 2-3 hours after inoculation and reached stationary phase around 7-9 hours (Figure 1A). Hall A sustained stationary phase for a longer period of time and started to show lysis after 20 hours, while ATCC 3502 started

Sporulation study

Bacterial cells were collected at designated time points for sporulation observation. Smears of the culture were prepared, heat fixed, and stained for the presence of spores by malachite green using the Schaeffer-Fulton staining method [27]. Images of stains were obtained using the Leica LAS EZ microscope (Buffalo Grove, IL). The presence of spores was also studied by examining the viability of bacterial culture after heat shock at 80 °C for 5 minutes.

Sequence analysis

The sequences and the annotated file of individual genes were retrieved from GenBank NC_009495 for *C. botulinum* ATCC 3502 and NC_009698 for Hall A (aka: Hall A-hyper). T-Coffee was used for multiple sequence alignment of the sporulation- and toxin-related genes. Notably, the FASTA sequence of CBO1120 was acquired for ATCC 3502 as well as the homologous sequence of Hall A. To align, these FASTA sequences were transferred to the T-Coffee Server found at.

lysis immediately after reaching its peak at 9-10 hours (Figure 1A). Similar growth curves were observed from two additional independent studies (data not shown). Based on this result, total RNA was extracted from cultures grown for 4, 6, and 8 hours to represent the mid-log, late-log, and early stationary phases of growth, respectively (Figure 1B).

Transcriptome analysis reveals differentially expressed genes between ATCC 3502 and Hall A

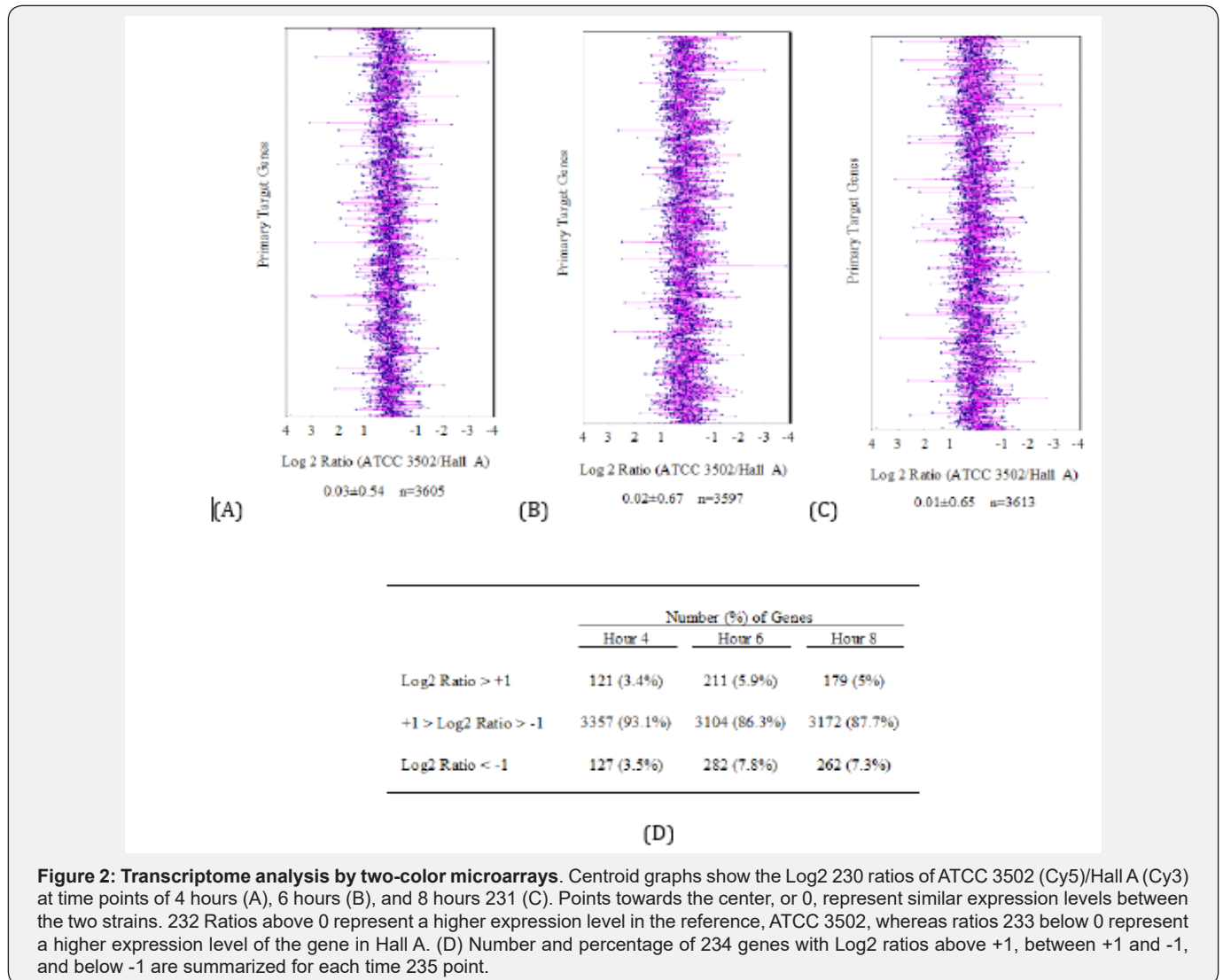


Figure 2: Transcriptome analysis by two-color microarrays. Centroid graphs show the Log₂ 230 ratios of ATCC 3502 (Cy5)/Hall A (Cy3) at time points of 4 hours (A), 6 hours (B), and 8 hours 231 (C). Points towards the center, or 0, represent similar expression levels between the two strains. 232 Ratios above 0 represent a higher expression level in the reference, ATCC 3502, whereas ratios 233 below 0 represent a higher expression level of the gene in Hall A. (D) Number and percentage of 234 genes with Log₂ ratios above +1, between +1 and -1, and below -1 are summarized for each time 235 point.

Two-color microarray analysis was used to compare the transcriptomes of *C. botulinum* ATCC 3502 and Hall A. The differential expressions of individual genes were presented as the Log₂ ratios of Cy5/Cy3 (ATCC 3502/Hall A). The results in Figure 2 show the centroid graphs across a range of -4 and +4 of the Log₂ ratios. It is clear that the majority (86.3 – 93.1%) of the genes show similar expression levels (within two-fold differences) between the two strains as demonstrated by the number of genes showing close to zero Log₂ ratios in all three time points studied (Figure 1d). However, there are distinctive differential expressions of some genes among the three sampling time points where slightly more differences were observed in the latter two time points. Genes found to be above a Log₂ ratio of +2 and below a Log₂ ratio of -2 were identified and listed in S1 Table. The total number of genes that were expressed by more than four-fold in ATCC 3502 than Hall A (using Log₂ ratios > 2) were 9, 8 and 19 for transcriptomes from 4, 6, and 8 hours of growth, respectively. While the numbers of genes that were expressed four times less in ATCC 3502 than Hall A (Log₂ ratios < -2) were 5, 13 and 16 for transcriptomes

from 4, 6, and 8 hours of growth, respectively. There is an increase in differentially expressed genes at hour 8, or the early-stationary phase, as compared to the other two sampling time points (Table 1a), suggesting that the two strains may be reacting differently while entering the stationary phase when the nutrient depletion and accumulation of toxic products occurred. CBO0278, a maltose-6-phosphate glucosidase, is the only gene to be shown at all three time points to have Log₂ < -2, indicating a higher expression level in Hall A over ATCC 3502. A similar behavior was seen in CBO2538, encoding for a hypothetical protein, with an exception t hour 4 where the expression level (Log₂ ratio = -1.98) was only slightly above our Log₂ cut-off at -2. It is worth noting that an anti-sigma F factor (CBO3088), which promotes the fore spore formation, was expressed more at hour 8 in ATCC 3502 than Hall A (Log₂ ratio at 2.32; Table1c), indicating lack of CBO3088 expression in Hall A despite a gene homolog present in Hall A (3,144,309 - 3,144,731). Overall, most of the genes that were over expressed in ATCC 3502 compared to Hall A are involved in carbohydrate transportation and catabolism (1a, 1b, and 1c Tables), suggesting a need of

energy and substrates for active growth and/or sporulation. Most of the genes that were under-expressed in ATCC 3502 are related

to anaerobic respiration (1d, 1e, 1f Tables), suggesting a possible switch of the energy source in Hall A to deter from sporulation.

Table 1a: Supplemental.

Locus Tag on ATCC 3502	Primary Target	Cy5 Intensity (ATCC 3502)	CY3 Intensity (Hall A)	Log2 Ratio $\frac{ATCC3502}{HallA}$	Hornologs in Hall A?	% Ideality
CB00975	Dihydroxyacetone kinase	61031	6177	3.3	Yes	2289/2289 (100%)
CB00976	Glycerol dehydrogenase	20943	2354	115	Yes	1471/1471 (100%)
CB02875	Phosphoribosylformylglycinamide cyclo-ligase	16424	1846	115	Yes	1307/1307 (100%)
301100	Putative sodium: tinc symporter	4656	612	193	Yes	1817/1818 (99%)
CB02876	Amidophosphoribosyltransferase precursor	13720	2146	2.68	Yes	1883/1883 (100%)
CB02864	Riboflavin biosynthesis protein rfi3a	11680	1892	2.63	Yes	1568/1568 (100%)
CB02866	Riboflavin biosynthesis protein rbd tra reductase	8183	1757	2.22	Yes	1872/1872 (100%)
CB02000	Methyl-accepting chemotaxis protein	1023	221	221	Yes	2144/2144 (100%)
CB02878	Phosphoribosylaminoimidazole carboxylase catalytic subunit	7947	1817	2.13	Yes	874/874 (100%)

Table 1b: Hour 6, Log2 ratios > +2.

Locus Tag on ATCC 3502	Primary Target	Cy5 Intensity (ATCC 3502)	Cy3 Intensity (Hall A)	Log2 Ratio $\frac{ATCC3502}{HallA}$	Hornologs in Hall A?	% Identity
CB00231	Probable protein-export membrane protein	1060	142	2.9	Yes	302804 (99%)
CB03241	Aspartate carbamoyltransferase catalytic chain	4171	587	2.83	Yes	1200/1200 (100%)
CB01991	PTS system, Ilbc component	11598	1660	2.8	Yes	1818/1818 (100%)
CB00975	Thydroxyacetone kinase	14935	2262	172	Yes	2289/2289 (100%)
CB00976	Glycerol dehydrogenase	4173	770	2.44	Yes	1471/1471 (100%)
CB03328	Putative phosphatase	1172	254	2.21	Yes	1291/1291 (100%)
CB03300	Putative integral membrane protein	1312	322	2.03	Yes	839/839 (100%)
CB03237	Dihydroorotate dehydrogenase electron transfer subunit	3887	953	103	Yes	982/982 (100%)

Table 1c: Hour 8, Log2 ratios > +2.

Locus Tag on ATCC 3502	Primary Target	CY5 Intensity (ATCC 3502)	Cy3 Intensity (Hall A)	Log2 Ratio $\frac{ATCC3502}{HallA}$	Hornologs in Hall A?	% Identity
CB01991	PTS system Ilk component	75560	4811	3.97	Yes	1818/1818 (100%)
CB01992	Probable sugar kinase	9806	959	3.35	Yes	1200/1200 (100%)
CB01990	PTS system. Ila component	21704	2279	3.25	Yes	592/592 (100%)

CB02150	Putative sugar transporter	119924	12725	3.24	Yes	17751/1775 (100%)
CB01993	Tagatose-1,6-bisphosphate aldolase	19324	2409	3	Yes	L119/1119(100%)
CB01068	Putative anaerobic glycerol-3-phosphate dehydrogenase submit a	13383	1704	2.97	Yes	1845/1845 (LOD%)
CB02153	Putative transaldolase	14072	1836	2.94	Yes	931/931(100%)
CB02785	Glycerol uptake facilitator protein	22388	3279	2.77	Yes	917/917 (100%)
CB02151	Putative phosphotransferase system component	19174	2819	2.77	Yes	371/371(100%)
CB00345	Aldehyde-alcohol dehydrogenase	12068	1839	231	Yes	3359/3364 (99%)
CB02217	Putative sorbitol dehydrogenase	3361	536	2.65	No	significant similarity
CB01069	Putative pyridine nucleotide -disulphide osidoreductase	24982	4167	2.58	Yes	1633/1633(100%)
CB02152	Putative sugar phosphotansferase	64520	11712	2.46	Yes	570/570(100%)
CB01539	Putative proton'peptide *Importer family protein	9301	1797	2.37	Yes	18241/1824 (100%)
CB030813	Anti-sigma F factor	8193	1642	2.32	Yes	549/549 (100%)
CB01100	Putative sodium: alanine symporter	2877	646	2.15	Yes	1817/1818 (99%)
CB03324	Conserved hypothetical protein	42495	9732	2.13	Yes	530/530 (100%)
CB02730	Flagellin	12799	2932	2.13	Yes	1076/1076 (100%)
CB01847	Putative catalytic subunit of iron-only hydrogenise	12963	3073	2.08	Yes	2254/2254 (100%)

Table 1d: Hour 4, Log₂ ratios < -2.

Locus Tag on ATCC 3502	Primary Target	Cy5 Intensity (ATCC 3502)	Cy3 Intensity (Hall A)	Log ₂ Ratio $\frac{ATCC3502}{HallA}$
C1300278	rnahosc4'-phosphate glucosidase	338	5006	-3.89
CB01581	hypothetical protein	3126	22377	-2.84
CB01580	pyridine nucleotide-disulfide oxidoreductase	3968	23611	-2.57
CB03310	carbon starvation protein CstA	1577	9238	-2.55
C1300612	hypothetical protein	5738	25180	-2.13

Table1e: Hour 6, Log₂ ratios < - 2.

Locus Tag on ATCC 3502	Primary Target	Cy5 Intensity (ATCC 3502)	Cy3 Intensity (Hall A)	Log ₂ Ratio $\frac{ATCC3502}{HallA}$
CB03310	carbon starvation protein CstA	279	4495	-4
CB00278	maltose-6'-phosphate glucosidase	519	4111	-2.99
CB02864	bifunctional riboflavin biosynthesis protein RibAB	2128	11417	-2.42
CB02863	6,7-dimethyl-8-ribityllumazine s! mthase	1085	5233	-2.27
CB00106	radical SAM domain protein	372	1785	-2.26
CB02732	hypothetical protein	288	1326	-2.2
CB00478	cadmium-translocating P-type ATPase	467	210B	-2.17
CB00486	hypothetical protein	405	1806	-2.16

CB02729	glycosyltransferase	345	1542	-2.16
CB00236	hypothetical protein	2215	9842	-2.15
CB01900	hypothetical protein	371	1592	-2.1
CB02538	hypothetical protein	462	1955	-2.08
CB00801	ha 70	1274	5221	-2.03

Table 1f: Hour 8, Log2 ratios < -2.

Locus Tag on ATCC 3502	Primary Target	Cy5 Intensity (ATCC 3502)	Cy3 Intensity (Hall A)	Log2 Ratio $\frac{ATCC3502}{HallA}$
CB01331	oxidoreductase, acetyl-CoA syntbase subunit	2083	26377	-3.66
CB03310	carbon starvation protein estj;	4070	27844	-2.77
CB02538	hypothetical protein	274	1875	-2.77
CB0478	cadmiumaanslocating P-type ATPase	831	5202	-2.65
CB02196	acvl-CoA deb) drogenase	401	2418	-2.59
CB02198	subunit of oxygen-sensitive 2-hydroxyisocaproyl-CoA dehydratase	13 L6	6645	-2.34
CB02195	electron transfer flavoprotein subunit beta	926	4601	-2.31
CB02222	(4Fe-4S) - binding protein	1189	5853	-2.3
CB02732	hypothetical protein	375	1787	-2.25
CB00278	maltose-6'-phosphate glucosidase	880	4320	-2.3
CB00476	hypothetical protein	582	2754	-2.24
CB03462	50S ribosomal protein L15	21771	96012	-2.14
CB03214	rubredoxinfrubrerydrin	11275	48968	-2.12
CB03459	methionine arrimpeptidase	5858	25172	-2.1
CB01329	hypothetical protein	970	4135	-2.1
CB02199	isocaprenoyl-CoA: 2-hydroxy isocaproate CoA-transferase	865	3478	-2

Transcriptome profiles confirm Hall A as a high toxin producer

The expression patterns of the toxin cluster genes (CB00801 – CB00806) were examined between ATCC 3502 and the homologs in Hall A. When graphing the individual dye intensities, ha17, ha33, ha70, ntnh, and bont show similar increasing expression trends for both strains where the expression was the highest at hour 8 (early stationary) among the three time points analyzed (Figures 3A-C, 3E, & 3F). Despite the similar expression patterns, Hall A did display slightly higher intensities at hours 6 and 8 for bont and ha genes while ntnh expression patterns were similar between the two strains (Figs. 3A-C, 3E, and 3F). The temporal expression pattern of bot/R, the gene for a positive transcriptional regulator, is different from the other toxin cluster genes in that its expression in ATCC 3502 increased only slightly in the time study as compared to Hall A (Figure 3D).

The botR in Hall A showed a slight increase at hour 8 (Figure 3D), which appears to correlate to its higher toxin expression at later time points (Figure 3F). The expression of a two-component

system, CB00786/0787, a potential negative regulatory system for the toxin cluster was also observed to confirm its regulatory influence [18]. The two-component system is located at 888,856 – 890,985 in ATCC 3502, 10,896 bp upstream of the toxin cluster (Figure 3J). Both genes showed an upwards expression trend in ATCC 3502 and a down-and-up trend for Hall A (Figs. 3G and 3H). Although the expression levels were low in both strains as expected at the time points analyzed, the steadily increased expression levels of CB00786/0787 in ATCC 3502 may eventually contribute to the suppression of the neurotoxin expression, while the lack of the trend or delayed expression of this system in Hall A may contribute to its hyper toxin phenotype. A hierarchical cluster shows that the expression patterns of the regulatory genes, botR and CB00786/0787, are clustered in a separate clade from the ha and ntnh-bont operons, which further confirms that it is expressed differently than the other genes (Figure 3I). The majority of expression patterns show green heat maps throughout the time points for all toxin cluster genes (Figure 3I), which is not surprising since Hall A is known to be a hyper toxin producer than most other serotype A strains. The most distinctive green colored

heat maps are found for genes in the ha operon (ha33, ha17, ha70), especially ha33 and ha70 around hour 6 during the late-log growth phase, indicating a much higher level of expression was occurring in Hall A. Overall, our microarray analysis of the transcriptomes

not only provides the molecular evidence to support the hyper toxicity phenotype of Hall A [28]. It also provides further insights of gene regulation of the neurotoxin gene cluster between the two subtype A1 strains.

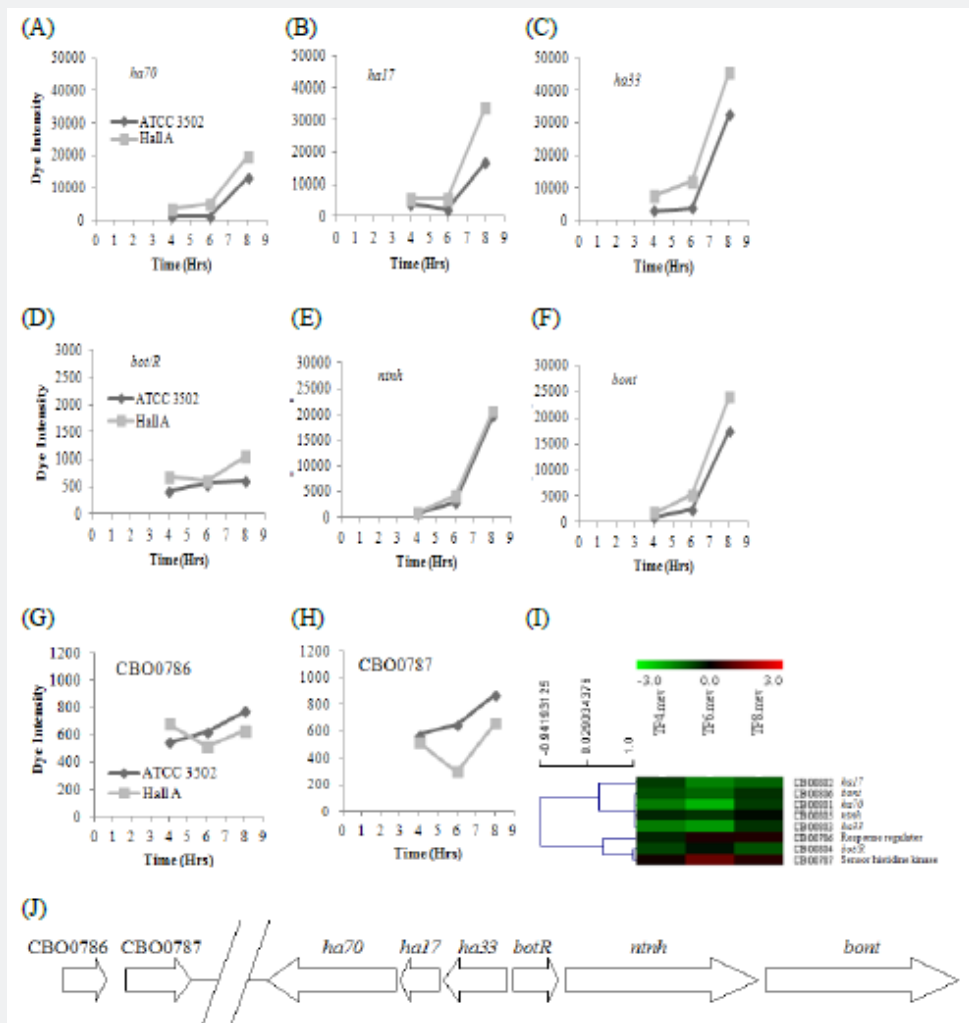


Figure 3: Heat map and dye intensities showing the expression of genes of the neurotoxin 282 cluster and relevant regulatory genes. Individual dye intensities were plotted against the three 283 time points for (A) ha70 (CBO0801), (B) ha17 (CBO0802), (C) ha33 (CBO0803), (D) bot/R 284 (CBO0804), (E) ntnh (CBO0805), (F) bont (CBO0806), (G) CBO0786, and (H) CBO0787. (I).

Additionally, real-time RT-PCR was used to confirm the expression patterns of bont, and the results showed comparable trends to that of the microarray data (data not shown). Heat map and clustering view of gene expression based on Log2 ratios. Heat maps in red color indicate higher levels of expression in ATCC 3502 (Cy5), whereas the green indicates more expression in Hall A. Heat maps in black color represent genes that were equally expressed in both strains. Heat map was constructed using complete linkage of Pearson Correlation using MeV of the TM4 Suite Software. (J) A representation of the neurotoxin gene cluster shows arrangement of selected genes studied.

Sporulation genes are more expressed in ATCC 3502 than Hall A

C. botulinum strain Hall A is known for its low or lack of sporulation. Sporulation patterns were compared among strains

ATCC 3502, Hall A, and NCTC 2916 during a 120-hour period (Figure 4). NCTC 2916 was added as a control for fast sporulation. Based on spore staining and microscopy, spores can be found in NCTC 2916 as early as 24 hours, as opposed to 108 hours in ATCC 3502. No spore production was observed in Hall A through the 120 hours analyzed (Figure 4). To further confirm if spores are absent in Hall A, cultures grown in TPGY broth for various time courses were sampled and heat shocked at 80 °C for 5 minutes, followed by a viability check. Hall A culture did not survive the heat shock even after 19 days of growth in TPGY, while NCTC 2916 and ATCC 3502 culture survived heat shock after 0 and 24 hours of growth, respectively (data not shown). Strain NCTC 2916 survived the heat shock at 0 hour obviously owing to the spores in the inoculum carried over from the overnight culture. Vegetative cells stained red-pink, whereas spores stain green. Arrows indicate the first appearance of spores in the respective strains.

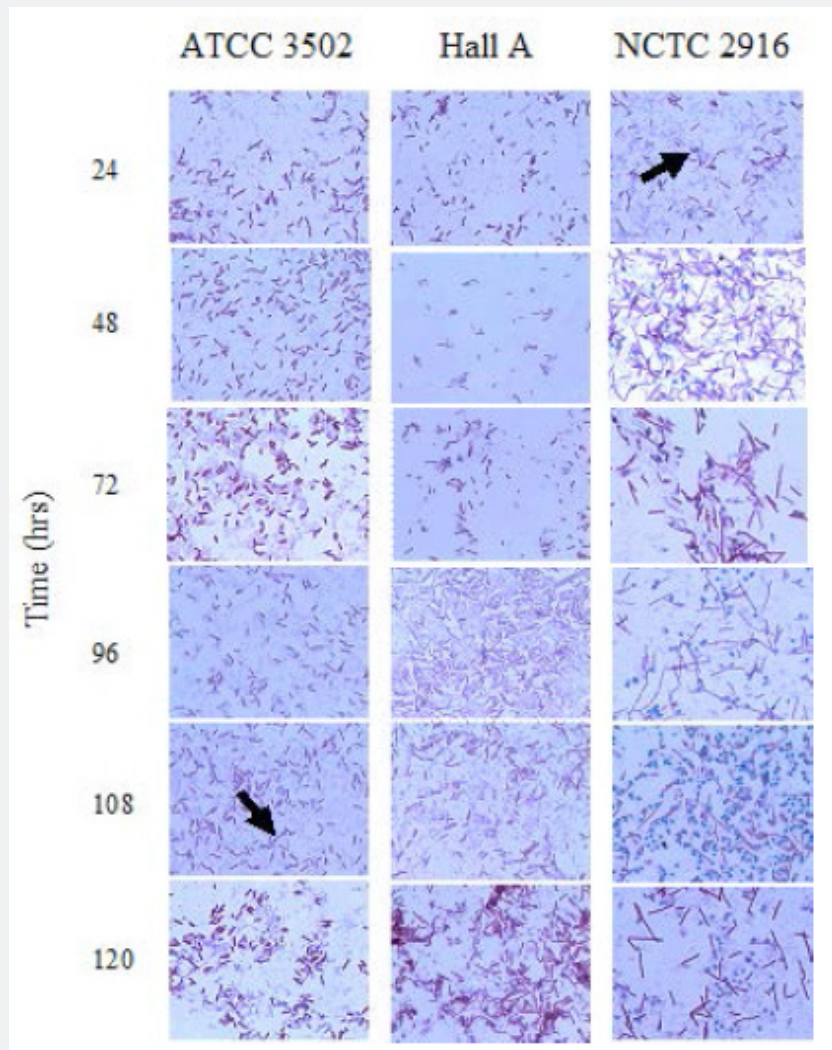


Figure 4: Spore stains of ATCC 3502, Hall A, and NCTC 2916 recovered at multiple time 306 points during the first 120 hours of growth.

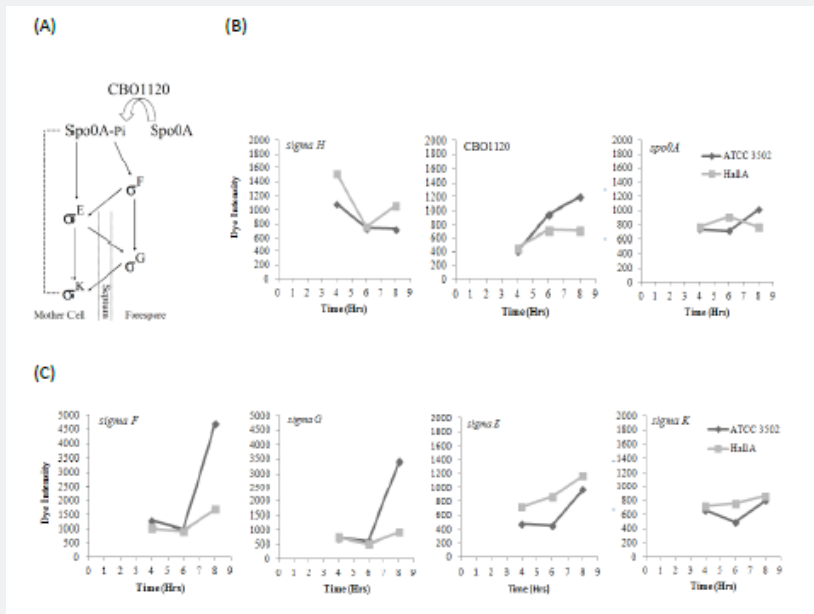


Figure 5: Expression patterns of selected key sporulation genes.

To further compare the differential sporulation processes in these two strains, the expression patterns for genes coding for the key regulatory molecules in the sigma cascade of sporulation, including Spo0A, Sigma H, Sigma E, Sigma F, Sigma G, Sigma K, and a sensor histidine kinase (CBO1120), were plotted and analyzed in order to understand their pathway trends (Figure 5). As a guide, the sigma cascade was plotted based on the Bacillus system [29] and studies in *C. botulinum* [20, 22] (Figure 5A). Expression of sigma H was high for both strains at the early growth stage and decreases as incubation time increases (Figure 5B), suggesting its role in vegetative growth and the stimulation of spo0A during the earlier growth stages. However, expressions of sigma H in Hall A were down and then back up at hour 8, which may imply a transition back to the vegetative growth.

As shown in Figure 5B, spo0A expression was low in all three time points in Hall A but increased during late log phase in ATCC 3502. The lack of spo0A expression in Hall A may explain the sporulation deficiency observed in this strain. Sigma F and G, responsible for regulating genes important in forespore formation, exhibited increases in expressions during late log phase in ATCC 3502, but not in Hall A (Figure 5C). Interestingly, the expression of the mother cell-specific sigma factor, sigma E, was not impaired in Hall A and showed a similarly increasing trend as in ATCC 3502 (Figure 5C). Sigma K, a transcriptional regulator involved in spore maturation, displayed a low expression level in both ATCC 3502 and Hall A as expected for the time points analyzed (Figure 5C). Despite of the low expression level, the down-and-up trend of expression of sigma K in ATCC 3502 was also observed in a separate transcriptomes analysis where 7 time points from hours 3 to 11 were examined (unpublished data).

The expression levels were also analyzed for the putative sensor histidine kinase, CBO1120, which exhibited phosphorylating capabilities towards Spo0A [20]. Although signals are relatively lower compared to those aforementioned sigma-related genes, there is a higher dye intensity for strain ATCC 3502 than Hall A at hour 8 (Figure 5B). The differential expression of spo0A and CBO1120 in these two strains may imply that spo0A is not only poorly expressed in Hall A, its phosphorylation activation by the sensor histidine kinase may also be reduced as compared to the expression level in ATCC 3502 (Figure 5B). When aligning the sequences of spo0A and cbo1120 from ATCC 3502 to the homologs in Hall A, a 100% and 99% identity, respectively, was observed (data not shown). A single A to G nucleotide substitution at position 661 of cbo1120 was found when compared to its homolog, clc1171 in Hall A resulting in a

glutamic acid to lysine substitution at amino acid position 221 (Figure 6). Interestingly, the amino acid difference falls right in the critical dimer interface and is only 7 amino acids away from the histidine phosphorylation site (Figure 6). Cooksley et al. [19] has identified two putative agr quorum sensing systems in *C. botulinum* ATCC 3502 and demonstrated their roles in regulating sporulation and neurotoxin formation. To examine if these agr systems are differentially expressed in the two strains studied, genes of the two putative agr systems were analyzed (S1 Figure). The expression patterns of the two agr regions in the two *C. botulinum* show similar flat and low expression trends during the three time points sampled, except for CBO0331 and CBO0338 (agrB-2) where the expressions were high at hour 4 and low at hours 6 and 8 (S1 Figure).

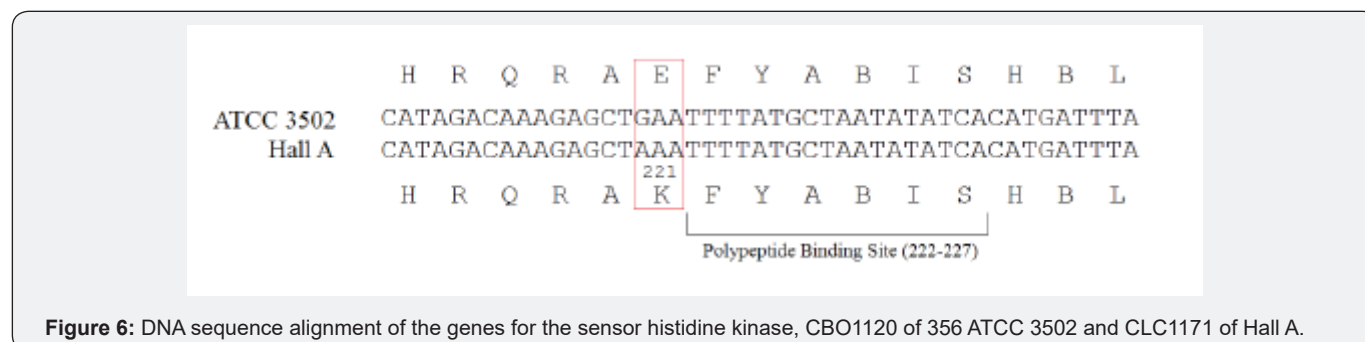


Figure 6: DNA sequence alignment of the genes for the sensor histidine kinase, CBO1120 of 356 ATCC 3502 and CLC1171 of Hall A.

Table 2: Supplemental.

	Locus Tag on ATCC 3502	Common Name	Hour4 ATCC3502	Hall A	Hour 6 ATCC3502	Hall A	Hour 8 ATCC3502	Hall A
σ^H	CBO1872	Spo0A*	737	765	713	908	1011	775
	CBO2403	SpoVS	32940	31184	22280	23855	27193	65669
	CBO2965	SpoIIF*	608	572	569	611	968	763
	CBO30139	SpoIIAA*	762	1019	772	800	1695	1061
	CBO3546	Spo VG	5070	4946	2346	5123	8006	12338

SPo0A	CBO1872	Spo0A*	717	765	715	908	1011	775
	CBO2532	Sigma G*	723	739	622	508	3411	912
	CBO2533	Sigma E	410	716	452	863	970	1162
	CBO2534	Spell GA	473	637	537	494	701	710
	CBO2965	Spoll F*	608	572	569	611	968	763
	CB03527	Spoll E	514	587	655	296	982	869
	C803087	Sigma F	1286	1023	970	925	4690	1692
	CB03088	Spoll AB	1683	1951	1478	1014	8193	1642
	CB03089	Spoll AA*	782	1019	771	800	1695	1061
σ^F	CB00126	Spo II R	170	1491	291	182	660	464
	CB001873	SpoI VB*	615	643	823	576	832	799
	CB002532	Sigma G*	723	739	623	508	3411	12
	CB03089	SpoII AA*	782	1019	772	800	1695	1061
	CB03537	Spo VT*	442	691	762	652	405	789
σ^G	CB01873	Spol VB*	625	613	823	576	532	799
	CBO2532	Sigma G*	723	739	622	508	3411	12
	CB03085	SpoVAD	2177	1523	784	798	2989	2842
	CB03089	Spoll AA*	782	1019	772	800	1695	1061
	CB03537	SPO VT*	442	691	762	652	405	789
σ^E	CB00035	BofA	1100	1000	993	540	980	718
	CB00160	SPOII D	852	564	766	651	818	804
	CB00162	span III D	440	657	496	840	649	1039
	CB01434	SPO VB	2232	1745	980	783	1507	1361
	CB01866	Spo IIM	538	403	900	509	864	807
	CB01888	Spo III AH	635	680	874	759	808	582
	CB01890	Spo III AF	1233	1438	588	1069	663	852
	CB01892	Spo III AD	724	534	756	701	794	829
	CB01893	Spo III AC	705	677	712	573	609	469
	CB01894	Spo III AB	973	1074	652	573	695	1005
	CB01895	Spo III AA	541	509	851	551	710	720
	CB01889	Spo III AG	756	954	571	552	1408	1200
	CB01891	Spo III AE	501	299	801	633	812	658
	CB02517	Spo I VA	1000	1135	824	794	1037	1302
	CB02541	Sigma K*	656	720	489	762	796	859
	CB02993	Spol VFB	829	505	667	613	766	834
	CB02993	Spo VB	703	515	843	572	1010	727
	σ^K	CB02541	Sigma K*	656	720	489	762	796

To further characterize the sporulation process, the transcriptome data of ATCC 3502 and Hall A was analyzed by pulling most of the sporulation related genes based on the annotated files from NCBI for ATCC 3502 (NC_009495) and Hall A (NC_009698). The genes were then sorted by the regulons based on the Bacillus system defined in SubtiWiki (<http://subtiwiki.uni-goettingen.de>). The dye intensities for both strains at each time point are included (Table 2).

None of these genes showed an extreme differential expression. The majority of regulons showed similar dye intensities for

both strains (Table 2), with the exception of a few genes which are highlighted in red and green to represent those with Log2 ratios higher than +1 and lower than -1, respectively (Table 2). Among the 32 genes analyzed, only five genes showed more than two-fold differential expressions. Four out of these five genes showed their differential expressions at hour 8 when the sporulation may be initiated in ATCC 3502. Among the four genes, only spoVS, an early gene induced by σ_H , showed a 2.4-fold higher expression level in Hall A; while three genes in the Spo0A regulon, sigG (CBO2532), sigF (CBO3087), and spoIIAB (CBO3088), showed higher ex-

pression levels in ATCC 3502, implicating a weakened or lack of activated Spo0A in the latter strain. Overall, based on the transcriptome analysis of ATCC 3502 and Hall A at mid-log, late-log, and early stationary growth phases, the differential expression occurred early in the initiation process as evident by the weak expression of spo0A and some genes in the Spo0A regulons in Hall A.

Discussion

Phenotypic variations were observed among the closely related *C. botulinum* subtype A1 strains, despite their similarity in genomic structure and gene functions [3,8]. Comparative genomic analysis of the assembled A1 genomes of *C. botulinum* ATCC 3502, ATCC 19397, and Hall A showed strong genomic alignments and a shared core of over 90% of their genes [3]. To further correlate the functions to their genomic contents, we compared the transcriptomes of two selected *C. botulinum* subtype A1 strains, ATCC 3502 and Hall A, with distinctive phenotypes in sporulation and neurotoxin production. *C. botulinum* ATCC 3502, the first *C. botulinum* genome being sequenced, produces modest levels of neurotoxin and endospores under normal laboratory conditions. Interestingly, the hyper toxin-producing strain Hall A, used in the commercial production of A1 neurotoxin for medicinal and research purposes, is known to be weak or lack in sporulation [28]. Our comparative analyses showed similar growth patterns (Figure 1) and transcriptomes (Figure 2) between ATCC 3502 and Hall A. The majority of the genes are expressed similarly with 93% of the genes falling within Log₂ of +1 during the mid-log growth phase and dropping to approximately 86% for late log and early stationary phase (Figure 2).

In this study, we verified that Hall A lacks the capability to form spores in our culturing condition even with extended incubation time, as evident by the absence of spores by microscopic spore staining (Figure 4; 120 hours) and inability to survive heat shock after 19 days. Not much is known of whether the hyper toxicity and lack of sporulation in Hall A strain are related or independent events. In *Bacillus subtilis*, the environmental cues are received and transmitted through a two-component system using multiple sensor kinases (KinA-E) that will auto phosphorylate on a conserved histidine residue. A phosphorelay will take place by passing the phosphate group sequentially to Spo0F, Spo0B, and finally the aspartate residue of Spo0A, the master regulator that turns on sporulation [29]. In *B. subtilis*, a promoter upstream of Spo0A is expressed at relatively low levels during mid exponential phase, under the control of σ A-RNA polymerase [30-34]. Upon exiting the exponential phase, the expression of σ H and phosphorylation of Spo0A, which is driven by KinA, controls a downstream promoter that sustains high levels of Spo0A and subsequently, sporulation [35]. The phosphorelay of Spo0A

In *Clostridium* is still unknown since Spo0F and Spo0B are absent from *C. botulinum* [20]. There are three proposed possibilities of Spo0A phosphorylation in *C. botulinum*, which include the existence of a different yet unknown phosphorelay system, direct phosphorylation by acetyl- or butyryl-phosphate, or direct phosphorylation by sensor kinases [36]. Similar sensor

histidine kinases were identified in *C. botulinum*. Among them, CBO1120 is the only one out of the 35 sensor histidine kinases in ATCC 3502 that is capable of phosphorylating Spo0A [20]. In our study, we found a higher level of expression of CBO1120 sensor kinase at hour 8 in ATCC 3502, but not in Hall A. When comparing the sequences of CBO1120 from ATCC 3502 with the homolog in Hall A, a G to A transitional mutation was found at nucleotide position 661 resulting in an amino acid substitution from glutamic acid to lysine, i.e. E221K (Figure 6). Interestingly, this substitution is located within the conserved dimer interface polypeptide binding motif of sensor kinases and is only seven amino acids away from the histidine phosphorylation site (H228). Further studies will be needed to determine if E221K modification has altered the subsequent phosphorylation of Spo0A. Interestingly, CBO1120 is closely related to orphan sensor histidine kinases, which are part of the two-component system. Three such orphan kinases, CBO0336, CBO0340, and CBO2762, have been identified in ATCC 3502. Our expression analysis showed that these three kinases were expressed at very low levels in both ATCC 3502 and Hall A during the time points we studied (S1 Figure and unpublished data). Further studies to measure CBO1120 kinase activity and its subsequent Spo0A phosphorylation and spore morphological changes in the two strains will be required to understand whether they may play a role in the triggering of sporulation in *C. botulinum*.

In *Bacillus subtilis*, the sigma cascade is triggered after the initiation of sporulation by phosphorylated Spo0A, starting with the activation of SigF which then activates SigE via SpoIIGA and SpoIIR. SigE will use SpoIIGA to activate SigG, which will finally activate SigK through SpoIVFB [29]. From our data, SigF and SigG, which are needed for subsequent forespore-specific sporulation processes, are highly expressed at hour 8 in ATCC 3502 but were severely lowered in Hall A (Figure 5C). This further demonstrated the absence or severely lowered expressions of forespore specific regulatory network in Hall A. On the other hand, the early mother cell specific regulator, SigE, was expressed at lowered levels but with an increasing trend in both strains (Figure 5C), suggesting that the forespore, but not the mother cell, regulatory network may have been compromised in Hall A strain resulting in its poor sporulation phenotype. Based on the *Bacillus* model, we believe the poor expression of Spo0A may have contributed to the lowered SigF and SigG expressions in Hall A at hour 8 and the SigE may be triggered by a small amount of SigF produced or an alternative regulatory pathway in Hall A. The sigma cascade of *C. botulinum* is not well-understood; however, it is probably different slightly from the system found in *B. subtilis*.

Recent studies have shown that these sporulation-specific sigma factors may have a role in early sporulation process in *C. botulinum* as demonstrated by the disrupted expression of Spo0A in the SigF, SigE, or SigG knockout mutants [23] and a biphasic expression of SigK in early and late growth phases [21,22]. Our data support the biphasic expression of SigK in ATCC 3502 (Figure 5C and unpublished data), but not in Hall A (Figure 5C). It is not clear whether the lack of the biphasic sigK expression in Hall contributed to its sporulation problem. We also observed severely

lowered expressions of *spo0A*, *sigF*, and *sigG* in Hall A (Figures 5B and 5C). Kirk et al [23] has shown that knockout of *SigF* or *SigE* prevents the formation of endospores, while *SigG* mutants did form spores but without a coat [23]. Studies on *spoIIID* knockout in *C. botulinum* type B has an impact on earlier genes like *Spo0A* and *SigF*, further confirming that sporulation differs between *C. botulinum* strains and *B. subtilis* [37]. The lack of spores in Hall A suggests that the sporulation was interrupted at a much earlier stage than the *SigG* (Figure 4). Further studies using knockout and/or over-expression 26 mutants, as well as electron microscopy, may be required to figure out the molecular mechanisms of sporulation deficiency in Hall A.

Our transcriptome analysis confirmed the temporal expression of genes in the HA+ toxin cluster of the two subtype A1 strains studied where these genes started to express at mid- to late-log growth phase (Figure 3) [9,10,17]. When comparing the two A1 strains, the expressions were slightly higher in Hall A as compared to ATCC 3502 (Figure 3), which may only partially account for the hyper toxin yield in Hall A (~3-10 folds). Comparable toxin yields, as determined by ELISA, were also observed between Hall A and a laboratory strain, 62A [9]. The results in both TPGY and TPM media showed only slightly higher toxin yields in Hall A during the first 24 hours. The hyper yield in Hall A (~ 3-fold higher) appeared to occur much later in growth (after 48 hours) and only in TPM medium [9]. Our microarray-based transcriptome analysis was limited to early growth stages where high quality RNAs could be obtained. Furthermore, the hyper toxicity in Hall A could be resulted from post-translation modifications in aged culture (after 48 hours) where the single chain inactive neurotoxin is nicked to the active di-chain form [9,10]. Despite that, we were able to compare the neurotoxin expression patterns during the early growth of the two A1 strains.

Our analysis of *BotR*, a positive regulator of the bi- and tri-cistronic *bont* and *ha* operons, shows an expression pattern distinctively different from the rest of the genes in the toxin cluster (Figure 3B), which supports the fact that *BotR* expression is regulated under its own element [38]. Interestingly, Hall A strain did show a higher *BotR* expression level than ATCC 3502, supporting its positive regulatory role leading to the elevated expressions of *BoNT* and *HA* genes in Hall A (Figures 3A-F). More recently, Zhang et al. [18] identified a two-component regulatory system, CBO0787/0786, which is located ~11 kb upstream of the HA+ toxin cluster and appears to bind directly to the promoters and repress the expression of the *ntnh-botA* and *ha* operons [18]. In our study, CBO0786 and CBO0787 showed a steady increase in their expressions in ATCC 3502, but not Hall A, during the time points analyzed (Figures 3G&3H) [18]. The *cb0787* or *cb0786* mutants have shown to cause up to a 10-fold increase of the neurotoxin expression [18], which was much higher than what was observed in our study. We believe this two-component negative regulatory system was functioning in Hall A but was down-regulated slightly to allow only a modest increase in the expression of genes in the HA+ toxin cluster (Figures 3G and 3H).

The synchronization between neurotoxin production and sporulation has long been suspected, especially owing to the existence of the hyper toxin producer, Hall A, which lacks sporulation capability [28]. Two tandemly located *agrBD* loci were found in Group I *C. botulinum* and *C. sporogenes* and appear to act through quorum sensing to orchestrate the neurotoxin production or sporulation in the bacterial cells [19]. With the use of the *Clostron* knockouts and anti-sense RNA, the study was able to show the correlation of *agr-1* to sporulation and *agr-2* to neurotoxin production. These two *agr* loci and their surrounding genes were analyzed, and our results show no major differential expressions between Hall A and ATCC 3502 that could clearly explain the differential phenotypes between the two A1 strains (S1 Figure). We suspect the differential expression, if any, would take place at a later growth stage where quorum sensing is active (higher cell density). There is also a hypothesis suggesting that the repression of neurotoxin production and continuation into sporulation would be the metabolic controls due to limited nutrient and energy sources [18, 28]. Our transcriptome analysis of the highly differentially expressed genes ($\text{Log}_2 > 2$ or < -2) shows an overall trend of gene profile shift where most of the genes that were over expressed in ATCC 3502 are involved in carbohydrate transportation and catabolism and genes that were over-expressed in Hall A are related to anaerobic respiration (S1 Table). Such distinctive metabolic and energy pathway shift may be necessary for the bacteria to direct its resources to sporulation in ATCC 3502 and toxin production in Hall A.

Our transcriptome analysis of the two A1 strains provides strong evidence to show that the deficiency of sporulation in Hall A occurs early in the sporulation process, as shown by the lowered expressions of the putative signaling sensor histidine kinase, CBO1120, and the sporulation master regulator, *spo0A* in Hall A strain. Consequently, forespore-specific *SigF* and *SigG* were also severely impaired in Hall A. We also observed a slight increase of *BotR*, the positive regulator for the toxin cluster, and a slight decrease of the negative regulator, CBO0786/CBO0787, in Hall A, which may partially account for the higher toxin yield in Hall A.

Analysis of cells collected from later growth stages may be required to identify additional factors contributing to its increasing toxicity in the aged culture of Hall A. Such studies could be achieved using RNA-seq for transcriptome analysis and biochemical analysis to investigate post-translational modifications. To our knowledge, this study is the first transcriptome analysis to compare two *C. botulinum* subtype A1 strains with distinctive toxin production and sporulation phenotypes. Our study has shed light on the differential expression of these two strains for their global trends as well as selected individual key molecules, which will lead to further studies on individual molecules and pathways. Our findings set a foundation for further studies involving the use of knockout and/or over-expression mutants of genes important in the differential regulation of sporulation and toxin synthesis to help elucidate the regulation of sporulation and neurotoxin production in *C. botulinum*.

Acknowledgement

The authors would like to thank Dr. Eric A. Johnson of University of Wisconsin-Madison for providing the bacterial strain, Drs. Ren-Jang Lin and Carlotta Glackin of Beckman Research Institute of the City of Hope for their assistance in the microarray study, the Pathogen Functional Genomics Resource Center of J. Craig Venter Institute for the microarray slides, and DOE Joint Genomic Institute for the workshop on genomic analysis tools. This project is partially funded by NIH grant 1SC3GM086303.

References

1. Popoff MR, Bouvet P (2013) Genetic characteristics of toxigenic Clostridia and toxin gene evolution. *Toxicon* 75: 63-89.
2. Hill KK, Smith TJ, Helma CH, Ticknor LO, Foley BT, et al. (2007) Genetic diversity among botulinum neurotoxin-producing clostridial strains. *Journal of Bacteriology* 189(3): 818-832.
3. Ng V, Lin W-J (2014) Comparison of assembled *Clostridium botulinum* A1 genomes revealed their evolutionary relationship. *Genomics* 103: 94-106.
4. Hill KK, Smith TJ (2013) Genetic diversity within *Clostridium botulinum* serotypes, botulinum neurotoxin gene clusters and toxin subtypes. *Curr Top Microbiol Immunol* 364: 1-20.
5. Dineen SS, Bradshaw M, Johnson EA (2003) Neurotoxin gene clusters in *Clostridium botulinum* Type A strains: sequence comparison and evolutionary implications. *Current Microbiology* 46: 345-352.
6. Jacobson MJ, Lin G, Raphael B, Andreadis J, Johnson EA (2008) Analysis of neurotoxin cluster genes in *Clostridium botulinum* strains producing botulinum neurotoxin serotype A subtypes. *Appl Environ Microbiol* 74(9): 2778-2786.
7. Jovita MR, Collins MD, East AK (1998) Gene organization and sequence determination of the two botulinum neurotoxin gene clusters in *Clostridium botulinum* Type A(B) strain NCTC 2916. *Current Microbiology* 36(4): 226-231.
8. Fang P-K, Raphael BH, Maslanka SE, Cai S, Singh BR (2010) Analysis of genomic differences among *Clostridium botulinum* type A1 strains. *BMC Genomics* 11: 725.
9. Bradshaw M, Dineen SS, Maks ND, Johnson EA (2004) Regulation of neurotoxin complex expression in *Clostridium botulinum* strains 62A, Hall A-hyper, and NCTC 2916. *Anaerobe* 10(6): 321-333.
10. Rao S, L. SR, Morris M, Lin W-J (2007) Variations in expression and release of botulinum neurotoxin in *Clostridium botulinum* Type A strains. *Food borne Pathogens and Disease* 4(2): 201-217.
11. Leyer GJ, Johnson EA (1990) Repression of toxin production by tryptophan in *Clostridium botulinum* type E. *Arch Microbiol* 154(5): 443-447.
12. Patterson-Curtis SI, Johnson EA (1989) Regulation of neurotoxin and protease formation in *Clostridium botulinum* Okra B and Hall A by arginine. *Appl Environ Microbiol* 55(6): 1544-1548.
13. Connan C, Deneve C, Mazuet C, Popoff MR (2013) Regulation of toxin synthesis in *Clostridium botulinum* and *Clostridium tetani*. *Toxicon* 75: 90-100.
14. Marvaud J-C, Eisel U, Binz T, Niemann H, Popoff MR (1988) TetR is a positive regulator of the tetanus toxin gene in *Clostridium tetani* and is homologous to BotR. *Infect Immun* 66(12): 5698-5702.
15. Marvaud JC, Gibert M, Inoue K, Fujinaga Y, Oguma K, Popoff MR. botR/A is a positive regulator of botulinum neurotoxin and associated non-toxin protein genes in *Clostridium botulinum* A. *Molecular Microbiology*. 1998;29(4):1009-18.
16. Raffestin S, Dupuy B, Marvaud JC, Popoff MR (2005) BotR/A and TetR are alternative RNA polymerase sigma factors controlling the expression of the neurotoxin and associated protein genes in *Clostridium botulinum* type A and *Clostridium tetani*. *Mol Microbiol* 55(1): 235-249.
17. Connan C, Brueggemann H, Mazuet C, Raffestin S, Cayet N, et al. (2012) Two-component systems are involved in the regulation of botulinum neurotoxin synthesis in *Clostridium botulinum* type A strain Hall. *PLoS One* 7(7): e41848.
18. Zhang Z, Korkeala H, Dahlsten E, Sahala E, Heap JT, et al. (2013) Two-component signal transduction system CBO0787/CBO0786 represses transcription from botulinum neurotoxin promoters in *Clostridium botulinum* ATCC 3502. *PLoS Pathog* 9(3): e1003252.
19. Cooksley CM, Davis IJ, Winzer K, Chan WC, Peck MW, et al. (2010) Regulation of neurotoxin production and sporulation by a putative agrBD signaling system in proteolytic *Clostridium botulinum*. *Appl Environ Microbiol* 76(13): 4448-4460.
20. Worner K, Szurmant H, Chiang C, Hoch JA (2006) Phosphorylation and functional analysis of the sporulation initiation factor Spo0A from *Clostridium botulinum*. *Mol Microbiol* 59(3): 1000-1012.
21. Kirk DG, Palonen E, Korkeala H, Lindstrom M (2014) Evaluation of normalization reference genes for RT-qPCR analysis of spo0A and four sporulation sigma factor genes in *Clostridium botulinum* Group I strain ATCC 3502. *Anaerobe* 26: 14-9.
22. Kirk DG, Dahlsten E, Zhang Z, Korkeala H, Lindstrom M (2012) Involvement of *Clostridium botulinum* ATCC 3502 sigma factor K in early-stage sporulation. *Appl Environ Microbiol* 78(13): 4590-4596.
23. Kirk DG, Zhang Z, Korkeala H, Lindstrom M (2014) Alternative sigma factors SigF, SigE, and SigG are essential for sporulation in *Clostridium botulinum* ATCC 3502. *80(16): (5141-5150)*.
24. Dahlsten E, Kirk D, Lindstrom M, Korkeala H (2013) Alternative sigma factor SigK has a role in stress tolerance of Group I *Clostridium botulinum* strain ATCC 3502. *Appl Environmental Microbiol* 79(12): 3867-3868.
25. Ferreira FA, Souza RR, de Sousa Moraes B, de Amorim Ferreira AM, Americo MA, et al. (2013) Impact of agr dysfunction on virulence profiles and infections associated with a novel methicillin-resistant *Staphylococcus aureus* (MRSA) variant of the lineage ST1-SCCmec IV. *BMC Microbiology* 13: 93.
26. Martin MJ, Clare S, Goulding D, Faulds-Pain A, Barquist L, et al. (2013) The agr locus regulates virulence and colonization genes in *Clostridium difficile* 027. *J Bacteriol* 195(16): 3672-3681.
27. Murray RGE, Doetsch RN, Robinow CF (1994) Chapter 2: Determinative and cytological light microscopy. In: P Gerhards (Ed.) *Methods for General and Molecular Bacteriology*. Washington D C: ASM Press.
28. Schantz EJ, Johnson EA (1992) Properties and use of botulinum toxin and other microbial neurotoxins in medicine. *Microbiological Reviews* 56(1): 80-99.
29. Higgins D, Dworkin J (2012) Recent progress in *Bacillus subtilis* sporulation. *FEMS Microbiol Rev* 36(1): 131-1448.
30. Talukdar PK, Olguín-Araneda V, Alnoman M, Paredes-Sabja D, Sarker MR (2014) Updates on the sporulation process in *Clostridium* species. *Research in Microbiology* 166(4): 225-235.
31. Durre P, Hollergschwandner C (2004) Initiation of endospore formation in *Clostridium acetobutylicum*. *Anaerobe* 10(2): 69-74.
32. Losick R, Stragier P (1992) Crisscross regulation of cell-type-specific gene expression during development in *B. subtilis*. *Nature* 355(6361): 601-604.
33. Chibazakura T, Kawamura F, Takahashi H (1991) Differential regulation of spo0A transcription in *Bacillus subtilis*: glucose represses promoter switching at the initiation of sporulation. *J Bacteriol* 173(8): 2625-32.

34. Mirouze N, Prepiak P, Dubnau D (2011) Fluctuations in spo0A transcription control rare developmental transitions in *Bacillus subtilis*. *PLoS Genetics* 7(4): e1002048.
35. Chastanet A, Losick R (2011) Just-in-time control of Spo0A synthesis in *Bacillus subtilis* by multiple regulatory mechanisms. *J Bacteriol* 193(22): 6366-6374.
36. Durre P (2011) Ancestral sporulation initiation. *Mol Microbiol* 80(3): 584-587.
37. Hosomi K, Kuwana R, Takamatsu H, Kohda T, Kozaki S, et al. (2015) Morphological and genetic characterization of group I *Clostridium botulinum* type B strain 111 and the transcriptional regulator spoIIID gene knockout mutant in sporulation. *Anaerobe* 33: 55-63.
38. Raffestin S, Christophe J, Marvaud C, Cerrato R, Dupuy B, Popoff MR (2004) Organization and *Anaerobe* 10: 93-100.



This work is licensed under Creative Commons Attribution 4.0 License
DOI: [10.19080/AIBM.2018.11.555822](https://doi.org/10.19080/AIBM.2018.11.555822)

Your next submission with Juniper Publishers will reach you the below assets

- Quality Editorial service
- Swift Peer Review
- Reprints availability
- E-prints Service
- Manuscript Podcast for convenient understanding
- Global attainment for your research
- Manuscript accessibility in different formats
(Pdf, E-pub, Full Text, Audio)
- Unceasing customer service

Track the below URL for one-step submission
<https://juniperpublishers.com/online-submission.php>